

## Multi-Harmonic Modes in W7-AS High-Beta Configurations

A. Weller, A. Werner, J. Geiger, C. Nührenberg, H. Thomsen, W7-AS Team

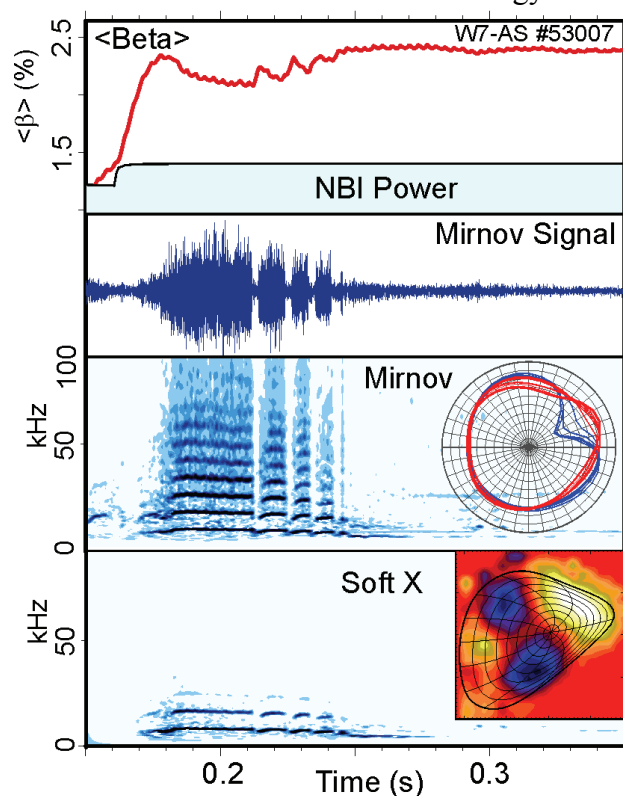
Max-Planck-Institut für Plasmaphysik, EURATOM Association, Greifswald, Germany

### Introduction

In the WENDELSTEIN W7-AS stellarator (1988-2002) very quiescent quasi-stationary high-beta plasmas up to  $\langle\beta\rangle = 3.4\%$  could be realised [1]. The maximum achievable beta is mostly determined by the available heating power rather than by MHD mode activity. A progressive deterioration of the equilibrium flux surfaces towards high  $\beta$  has been found to contribute to the  $\beta$ -saturation [2], but the global confinement does not show any significant degradation with respect to stellarator scaling laws. The absence of violent MHD activity close to the maximum achievable  $\beta$  has been attributed to self stabilisation effects due to pressure induced changes of the equilibrium (e.g. deepening of the magnetic well and increase of shear resulting from the Shafranov shift) [3], [4]. The results on W7-AS may be regarded as a first experimental confirmation of configuration optimisation which will be realised in W7-X to a large extent [5]. In this paper, we discuss some characteristics of MHD modes observed during the transition to high- $\beta$ .

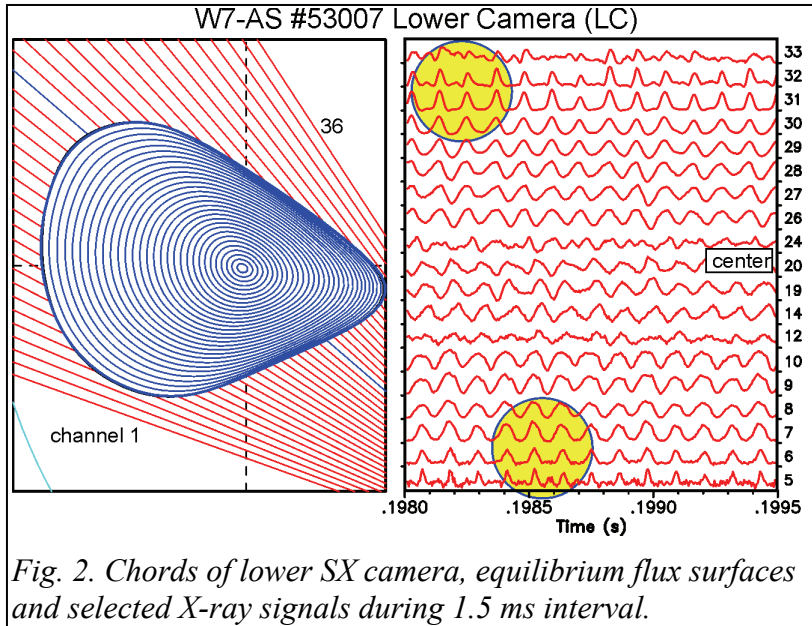
### Pressure driven low frequency modes during transition to high beta

Low frequency coherent modes are frequently seen in the range below  $\langle\beta\rangle \approx 2.5\%$ , mostly during the ramp-up phase of high- $\beta$  discharges. In many cases, this transient MHD activity, which is correlated with enhanced energy losses, exhibits two distinct features: (i) a frequency spectrum containing many harmonics



spectrum containing many harmonics (particularly in the data of the magnetic probes), and (ii) a pronounced ballooning behaviour. Fig. 1 shows a summary of discharge parameters and mode characteristics. The global radial and poloidal mode structure is deduced from tomographic reconstructions of the perturbed X-ray emissivity (8-10 cameras, up to 320 channels) [6] and from data of

*Fig. 1. Transient activity of pressure driven global modes dominated by  $(m,n) = (2,1)$ . The modes are correlated with a deterioration of the confinement. A strong ballooning effect is seen in the polar Mirnov amplitude diagram and the X-ray tomogram (insets)*



magnetic probe arrays using SVD methods (singular value decomposition). The ballooning could be related to the increase of the normal curvature in the good and bad curvature regions due to the Shafranov shift. The observation of higher mode harmonics in the raw signals resemble so-called Edge Harmonic Oscillations in tokamaks (EHO) [7], [8]

and Edge Harmonic Modes (EHM) in the Large Helical Device [9]. From fig. 2, where data of another X-ray camera system are shown, an increase of the harmonic content in the signals towards the plasma edge can be inferred (besides of channels close to phase inversions), and additional fine structure appears. These details can hardly be reconstructed by tomographic or standard magnetic analysis. Also, the magnetic signals often show a dominant in- outward oscillation rather than a poloidal rotation of the mode as found in the X-ray analysis. Therefore, a complementary approach was chosen based on mode simulations.

### Mode simulation model

The waveforms giving rise to the harmonic spectrum could be due to non-uniform mode rotation. However, a rigid and rather uniform rotation is inferred from the tomographic analysis. Also, a non-uniform rotation would impose a similar temporal dependence on all X-ray and magnetic signals as in the case of mode locking. Therefore, the harmonic spectrum is believed to originate from the spatial structure of the  $(m,n) = (2,1)$  mode (including the ballooning effect) and possibly from admixtures of mode harmonics with higher mode numbers  $m,n$ . In order to clarify this and the origin of sub-structures seen in particular channels of X-ray cameras and magnetic probe arrays we have performed simulation calculations using a heuristic model for a rotating radial mode displacement of the equilibrium flux surfaces. The 3-dimensional displacement is defined by a radial profile (effective flux surface radius) and a function, which is periodic in poloidal and toroidal directions on a magnetic angle grid, provided by the VMEC equilibrium reconstruction. The magnitude of the displacement along the poloidal circumference is adapted to satisfy  $\nabla \cdot \xi = 0$ . Additional parameters can be used for modelling of a ballooning effect so that the perturbation may be regarded as a superposition of a rotating contribution and a part oscillating inward-outward in

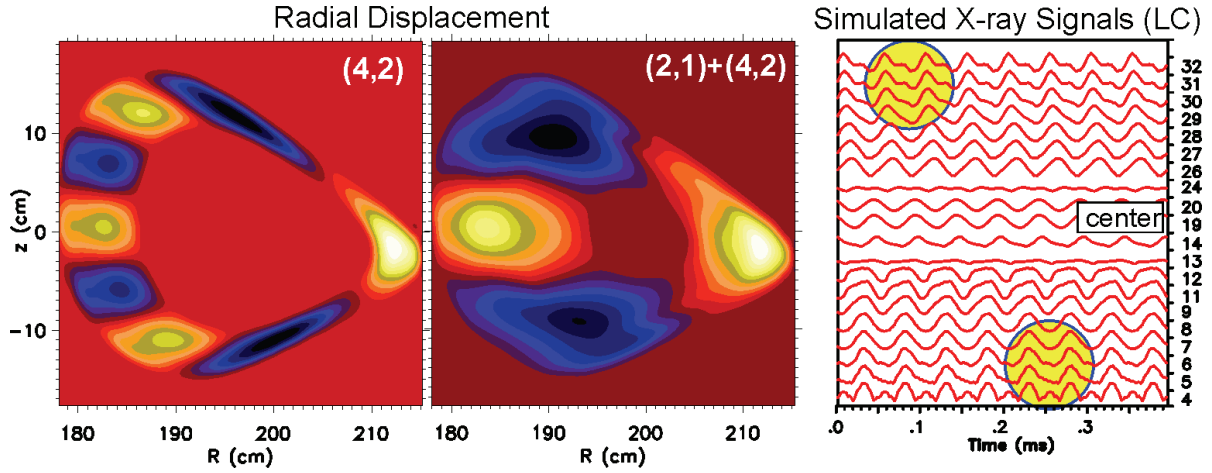


Fig. 3. Simulated X-ray signals with model for mixed (2,1) and (4,2) modes with ballooning

a fixed poloidal range. Then the displacement may analytically be represented by  $\xi = \xi_0(r, \theta) \cdot \exp[i(m\theta - n\phi - \omega t)]$ . If we use the Fourier expansion for the amplitude  $\xi_0(r, \theta) = \xi_{00}(r) + \sum_{j=1}^{j_{max}} \xi_{0j}(r) \exp(ij\theta)$ , one gets a harmonic spectrum with  $\omega = (m + j)\omega_{rot}$ , where  $\omega_{rot}$  is the rigid rotation frequency. In order to simulate the X-ray signals, a radial profile of the emissivity ( $\varepsilon_0(r)$ , constant on flux surfaces) is used, which is matched to fit the line integrated equilibrium profile. The simulated signals follow from line integrations over the perturbed emissivity  $\tilde{\varepsilon}(r, \theta, \phi)$  as a function of rotation angle, where  $\tilde{\varepsilon}(r, \theta, \phi) = -\xi(r, \theta, \phi) \cdot \partial \varepsilon_0(r) / \partial r$ . At the same time, Mirnov signals are simulated by using  $\tilde{\mathbf{B}} = \nabla \times (\xi \times \mathbf{B}_0)$ ,  $\tilde{\mathbf{j}} = 1/\mu_0 \nabla \times \tilde{\mathbf{B}}$  and a simplified version of Biot-Savart's law to calculate the perturbed magnetic field at the position of the probes. The poloidal perturbed magnetic field picked up by the magnetic probes is roughly proportional to the radial gradient of the displacement vector. In principle, the simulations allow to compare signals and their phase relations from different diagnostics and from different toroidal and poloidal locations.

In order to explain the intermediate peaks in the outer X-ray channels (highlighted in fig. 2) as well as in the time integrated Mirnov signals we first considered a tearing mode like displacement (radial eigenfunction with change of sign). Although the observed structure could be reproduced for particular channels, an additional phase reversal at slightly larger radius is generated by this displacement, which is in contradiction to the experimental data. We therefore considered kink-like displacements and the presence of two (or more) mode harmonics (see next section), which yields a reasonable agreement with the data (Fig. 3).

### Results from stability code calculations

A study of the global ideal mode analysis was made by the CAS3D code [10]. Unstable low-n modes have been found with growth rates of  $\gamma = 4.7 \cdot 10^4 \text{ s}^{-1}$  (fig. 4). As expected from the vicinity of the equilibrium to the rational  $\iota = 1/2$  surface, the (m,n) = (2,1) mode (N = 1

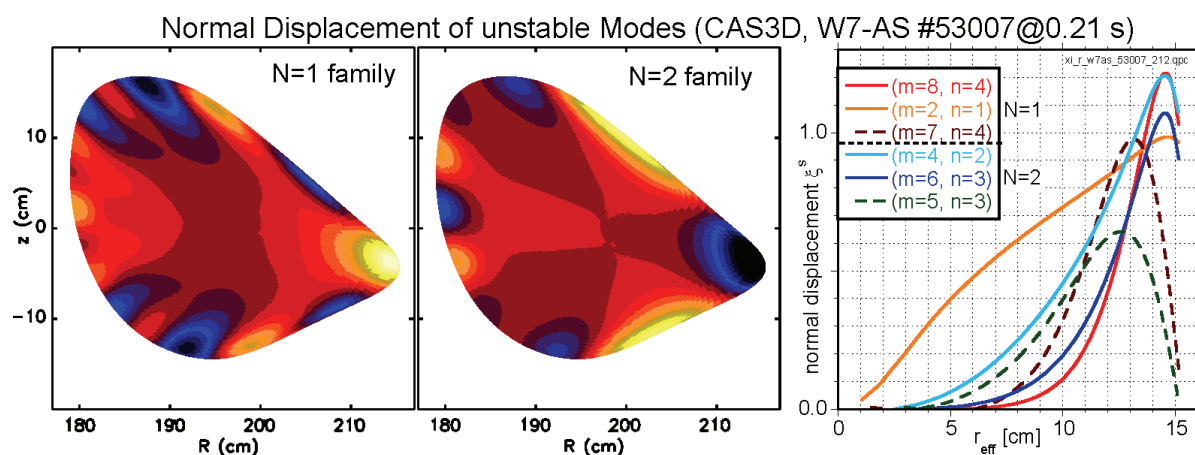


Fig. 4. Results of the computational analysis with the CAS3D MHD stability code.

family) has the most global structure. Together with the (4,2) mode (N = 2 family) and higher-n modes, which are localised closer to the plasma edge, the computational analysis yields a good agreement with the experimental data analysis including the observed ballooning behaviour. For slightly higher  $\beta$ , corresponding to the time after the mode activity shown in fig. 1, the growth rates are significantly lower. The modes are then more localised at the plasma edge, and in particular the (2,1) mode is not important anymore.

### Conclusions and summary

Global MHD modes in W7-AS high- $\beta$  plasmas have specific features. The presence of higher harmonics in the frequency spectra are caused by the spatial mode structure affected by the Shafranov shift and ballooning effects, as well as by admixtures of higher mode harmonics. Whereas the X-ray signals are proportional to the radial mode displacement, the magnetic signals are related to spatial and temporal derivatives of the displacement, which amplifies the harmonic content. At the toroidal position of the Mirnov probes the change between good and bad normal curvature along the horizontal midplane increases with  $\beta$  and is more pronounced than in the plane of the X-ray cameras. This may explain the dominating in-out ballooning oscillation found in the magnetic probe data. Most MHD modes are stabilised in configurations with good equilibrium properties and  $\langle \beta \rangle > 2.5\%$ .

### References

- [1] A. Weller, et al. *Plasma Phys. Control. Fusion* **45** (12A) A285-A308 (2003)
- [2] A. Reiman, et al. *Nucl. Fusion* **47**(7) 572-578 (2007)
- [3] A. Weller, et al. *32nd EPS Conf. on Plas. Phys., Tarragona*, **ECA Vol.29C** P-4.056
- [4] A. Weller, et al. *Fusion Sci. Technol.* **50** 158-170 (2006)
- [5] H. Wobig *Plasma Phys. Control. Fusion* **41** A159-A173 (1999)
- [6] C. Görner, et al. *24th EPS Conf. on Contr. Fus. & Plas. Phys., Berchtesgaden*, **21A** 1625
- [7] K. H. Burrell, et al. *Plasma Phys. Control. Fusion* **44** A253-A263 (2002)
- [8] W. Suttrop, et al. *Nucl. Fusion* **45** 721-730 (2005)
- [9] K. Toi, et al. *Nucl. Fusion* **44** 217-225 (2004)
- [10] C. Nührenberg *Physics of Plasmas* **6**(1) 137-147 (1999)